Analytical Biochemistry 428 (2012) 31–38

Contents lists available at SciVerse ScienceDirect

Analytical Biochemistry

journal homepage: www.elsevier.com/locate/yabio

Performance of fluorescent europium(III) nanoparticles and colloidal gold reporters in lateral flow bioaffinity assay

Etvi Juntunen *, Tiina Myyryläinen, Teppo Salminen, Tero Soukka, Kim Pettersson

Department of Biotechnology, University of Turku, 20520 Turku, Finland

ARTICLE INFO

Article history:
Received 12 April 2012
Received in revised form 31 May 2012
Accepted 5 June 2012
Available online 13 June 2012

Keywords:
Lateral flow assay
Time-resolved fluorescence
Europium nanoparticles
Colloidal gold
Point of care

ABSTRACT

Lateral flow (LF) immunoassays (i.e., immunochromatographic assays) have traditionally been applied to analytes that do not require very high analytical sensitivity or quantitative results. The selection of potential analytes is often limited by the performance characteristics of the assay technology. Analytes with more demanding sensitivity requirements call for reporter systems enabling high analytical sensitivity. In this study, we systematically compared the performance of fluorescent europium(III) [Eu(III)] chelate dyed polystyrene nanoparticles and colloidal gold particles in lateral flow assays. The effect of time-resolved measurement mode was also studied. Because binder molecules used in immunoassays might not behave similarly when conjugated to different reporter particles, two model assays were constructed to provide reliable technical comparison of the two reporter systems. The comparative experiment demonstrated that the fluorescent nanoparticles yielded 7- and 300-fold better sensitivity compared with colloidal gold in the two test systems, respectively. Although the two reporter particles may induce variable effects using individual binders, overall the high specific activity of Eu(III) nanoparticles has superior potential over colloidal gold particles for the development of robust high-sensitivity bioaffinity assays.

Lateral flow (LF)[1] immunoassays represent a popular and widely used test principle for point-of-care applications. The main features of LF tests are the user-friendly operation, quickly obtained results, and fairly good shelf life [1]. The easy assay procedure makes LF tests suitable for use by personnel without laboratory training and as over-the-counter products (e.g., for pregnancy and ovulation testing). However, there is an increasing need for high-performing LF-type tests in small laboratories and hospitals, emergency rooms, and doctor's offices. For rapid testing of cardiac troponins in the early triage of chest pain patients [2,3], currently available LF tests are highly insufficient. Several technical aspects of conventional LF tests contribute to the inadequate analytical performance, one being the low detectability of the traditionally used reporter option, the colloidal gold nanoparticle.

The gold(III) chloride nanoparticles were introduced for the first time as immunoassay reporters in a pregnancy hormone assay performed in microtiter wells [4]. Other visually detectable reporters, such as dyed latex and carbon nanoparticles, have been used in various LF applications [5]. Recently, more sophisticated methods have been implemented as LF assay reporter systems such as superparamagnetic beads [6,7], quantum dots [8], and upconverting phosphors [9]. Still, the majority of point-of-care LF tests rely on visual examination of a color-forming compound on the test strip, which constitutes a major and important advantage over test systems requiring an instrument-based readout. A visual readout, however, is prone to subjective interpretation of the test result. Poor lighting conditions (e.g., in an ambulance) may lead to false result interpretation. In addition, the use of a qualitative readout in the patient data records is unsatisfactory.

There are several reflectance- and fluorescence-based detection methods that enable data acquisition without subjective interpretation and are capable of quantitative measurements [5]. Fluorescence-based detection systems have been implemented in several successful LF tests [10–13]. Although the detection always requires special instruments, fluorescence-based assays have become widely used. For point-of-care applications, there are various types of handheld readers that are feasible for testing analytes with low sensitivity requirements. Currently, the majority of the fluorescent reporters in LF assays are detected by the specific emission wavelength of their short-lived fluorescence. A potential drawback in this is any background signal unrelated to the analyte itself (e.g., arising from the test materials and the biological sample). Therefore, the detection of low analyte levels may be compromised both by ambiguity of the signal formation and by low specific activity of the reporters.

* Corresponding author. Fax: +358 23338050.
E-mail address: etvi.juntunen@utu.fi (E. Juntunen).

[1] *Abbreviations used:* LF, lateral flow; Eu, europium; PSA, prostate-specific antigen; bio-BSA, biotinylated bovine serum albumin; BITC, biotin isothiocyanate; SA, streptavidin; Au, gold; UV, ultraviolet; SD, standard deviation; S/N, signal-to-noise.

0003-2697/$ - see front matter © 2012 Elsevier Inc. All rights reserved.
http://dx.doi.org/10.1016/j.ab.2012.06.005

Organic chelates of certain lanthanide ions (e.g., europium, terbium) have intrinsic fluorescence properties that can be used to produce high-activity reporters for diagnostic assays. Depending on the chelating structures and other synergistic components and conditions, these lanthanides exhibit variably long-lived fluorescence with a large and ion-specific Stokes shift. The slow decay of the fluorescence enables detection in a time-resolved manner, eliminating the short-lived background fluorescence of the test materials and biological materials. Europium(III) [Eu(III)] chelate dyed nanoparticles incorporate thousands of fluorescent chelates in a protective hydrophobic shell that results in chemical stability and high lanthanide-specific fluorescence [14,15]. Time-resolved measurement of fluorescent lanthanide chelates is an established method in high-sensitivity immunoassays [16–18]. More recently, successful use of Eu-doped nanoparticles on LF platforms has been demonstrated [11,19]. An LF assay using Eu(III)-loaded silica particles without time-resolved measurement reaching very high analytical sensitivity has been described [20]. However, direct comparative evaluations of novel versus traditional LF reporters have not been published.

In this study, two different model assays were constructed to compare the properties of Eu(III)-chelate-doped nanoparticles with colloidal gold reporters. A sandwich-type immunoassay to measure the free form of prostate-specific antigen (PSA) was chosen as the primary model assay. In the second model, the bioaffinity assay was constructed using streptavidin interaction with biotinylated bovine serum albumin (bio-BSA). The binders in the latter model assay are considered ideal in terms of the high binding affinity of biotin to streptavidin. The reactivity of binder molecules (e.g., antibodies) cannot be assumed to be unaffected after being conjugated to different reporter particles. Thus, the biotin–streptavidin model assay provides a comparison of the two reporter systems unaffected by possible changes of immunoreactivity on conjugation to the two different nanoparticles.

Thus, in this study, we systematically compared the detectability of fluorescent Eu(III)-doped polystyrene particles and colloidal gold particles. Three different methods for the readout of the fluorescent reporters were studied, and their respective capabilities to improve LF assays were compared. The fluorescence-based detection system was tested by using either a delayed time-resolved scanning mode or an instant measurement scanning without delay time between excitation pulse and measurement time window. In addition, a simple fluorescence imaging method using a digital camera was evaluated.

Materials and methods

Reagents and materials

BSA (Bioreba, Reinach, Germany) was covalently coupled with biotin isothiocyanate (BITC, University of Turku, Turku, Finland) to produce bio-BSA, a model analyte. The coupling reaction was performed in 50 mM carbonate buffer (pH 9.8) at 23 °C for 4 h. The concentration of BSA in reaction was 1 g/L, and BITC was used in 100-fold molar excess. Bio-BSA was separated from unbound BITC by NAP-5 and NAP-10 columns (Amersham Pharmacia Biotech, Uppsala, Sweden) using aqueous solution containing 0.9% NaCl. Carboxylate-modified Eu(III)-chelate-doped OptiLink polystyrene nanoparticles with 107 nm diameter (Seradyn, Indianapolis, IN, USA) were covalently linked with streptavidin (SA, Bio-SpA, Milan, Italy) or anti-PSA antibody 5A10 [21] as described by Kokko et al. [15] and Soukka et al. [22] to produce Eu(III)–streptavidin particles (SA–Eu) or Eu(III)–anti-PSA particles (anti-PSA–Eu).

SA-conjugated colloidal gold particles (SA–Au) with a diameter of 40 nm and an optical density of 10.3 AU at 520 nm (product code BA.STP40) were purchased from British Biocell International (Cardiff, UK). The anti-PSA antibody 5A10 was conjugated to colloidal gold (Ani Biotech, Vantaa, Finland) to produce Au–anti-PSA particles (anti-PSA–Au). The antibodies were diluted in MQ water to a concentration of 0.188 mg/ml and 100 μl of 200 mM sodium borate buffer (pH 9.0) to a total volume of 1 ml. The buffered antibody dilution was added to 5 ml of colloidal gold solution. The gold solution was previously adjusted to pH 9.0 with 20 mM K_2CO_3. The reaction was incubated overnight at 40 °C, and 5% BSA was added to block any free binding sites on particles. Excess antibodies were washed by centrifuging for 30 min with 15,000*g* at 4 °C and resuspending the pellet in 5 ml of 20 mM sodium borate buffer (pH 9.0) with 1% BSA. The washing step was repeated twice, and the final resuspension was done in 5 ml of the same buffer. The optical density at 520 nm was measured from the gold solution with a Shimadzu UV-1700 PharmaSpec spectrophotometer (Shimadzu, Germany).

The binder immobilization of bio-BSA assay strips was done by dispensing 4 g/L SA in 10 mM citrate–phosphate buffer (pH 5.0) with 1% methanol on nitrocellulose membrane (Hi-Flow Plus HF180, Millipore, Bedford, MA, USA). For PSA assay, the striping of the test line was done with anti-PSA antibody H117 (University of Turku) in a concentration of 1.5 g/L in 10 mM Tris–HCl buffer (pH 8.0) with 1% methanol. The control line was striped on the PSA strips at a 6-mm distance of the test line with rabbit–anti-mouse polyclonal antibody (Dako, Denmark) in a concentration of 0.4 g/L in the same buffer as described previously with SA striping. The striping applicator was adjusted to produce 1-μl/cm stripes with a liquid flow speed of 250 nl/s.

Prior to striping, the nitrocellulose membrane was attached to backing plastic with an adhesive surface (G&L Precision Die Cutting, San Jose, CA, USA). After the striping, membranes were dried at 35 °C for 1 h. An absorption pad was made by attaching a 40-mm-wide cellulose membrane strip (Millipore) to overlap 2 mm with nitrocellulose. A feeding pad of an 8-mm-wide glass fiber strip (Millipore) was attached to overlap 2 mm with the other end of the nitrocellulose. The assembled membrane card was cut in 4-mm strips (Fig. 1). The reaction buffer was 100 mM Hepes (pH 7.4) with 270 mM NaCl, 1% (w/w) BSA, and 0.5% Tween 20.

Instruments

The binder molecule striping was done with a Linomat 5 sample applicator (CAMAG, Muttenz, Switzerland). The test strips were cut with a desktop paper cutter (Ideal 1058, Krug & Priester, Balingen, Germany). A Victor X4 multilabel reader (PerkinElmer, Waltham, MA, USA) was used to measure the time-resolved fluorescence of Eu(III) nanoparticles (Fig. 2). A special frame was constructed to fit the LF test strips to a standard plate holder. The reflectance measurement of colloidal gold was done with a USB flatbed scanner (Canoscan 9900F, Canon, Tokyo, Japan). The fluorescence imaging was done with a Canon Powershot SX130 IS digital camera (Canon) and a D615/25 bandpass filter with a 25-mm diameter (Chroma, Bellows Falls, VT, USA). A handheld ultraviolet (UV) lamp (Spectroline, Westbury, NY, USA) with 254- and 365-nm wavelength lamps was used as an excitation light source.

Assay procedure

A standard series of analytes (bio-BSA, 5 pg/ml to 1 μg/ml; PSA, 5 pg/ml to 0.1 μg/ml) were diluted in reaction buffer. The reporters were also diluted in reaction buffer. SA–Au was diluted 1:1 to an optical density (520 nm) of 5, SA–Eu and anti-PSA–Eu to a concentration of 5×10^4 particles/μl. Standard dilutions of the analytes, solution of reporter-reagents, and reaction buffer for washing were applied in the wells of a polypropylene 96-well plate (cat. no.

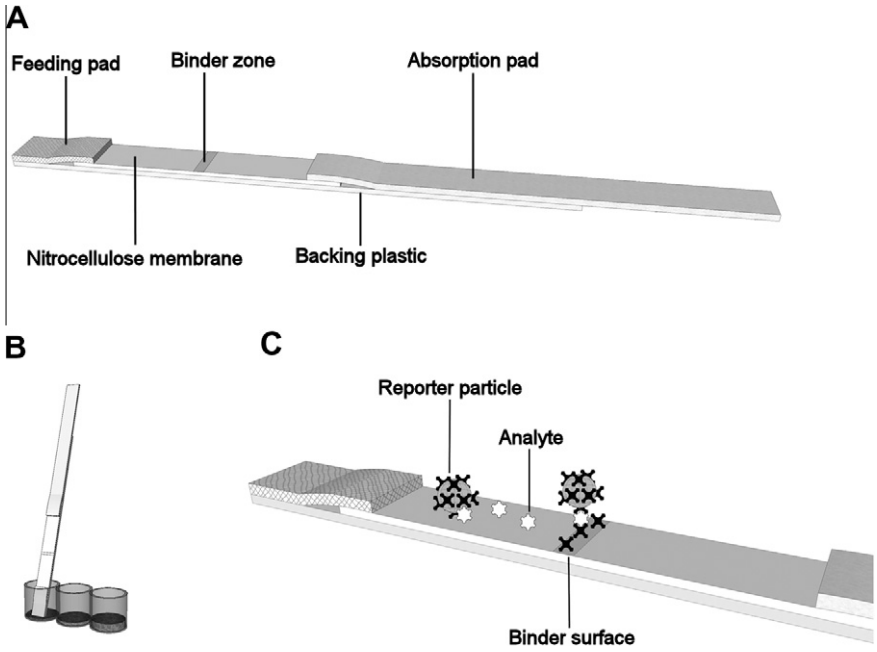

Fig.1. Schematic illustrations of the test strip (A), liquid absorbing procedure (B), and sandwich-type assay principle (C).

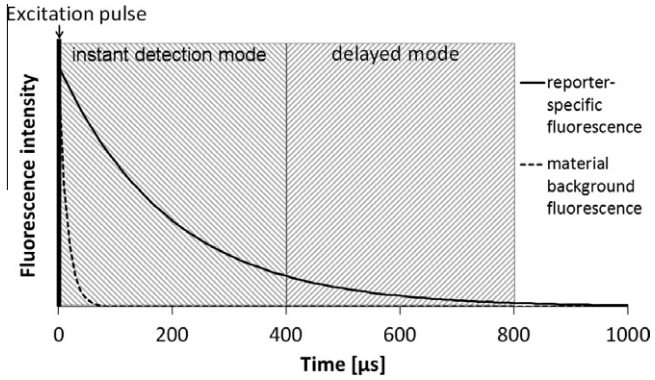

Fig.2. Illustration of the modes used for time-resolved measurement of Eu(III) nanoparticles. Nondelayed measurement at 0 to 400 µs also includes short-lived background fluorescence (dashed line). In the delayed measurement window, only long-lived fluorescence originating from the reporters (solid line) can be measured.

655201, Greiner Bio-One, Frickenhausen, Germany). Test strips were sequentially dipped in reagent solutions to absorb liquids on the strips (Fig. 1B). Volumes of the analyte solution and reporter solution in assay were 20 µl each. Washing of excess Eu(III) reporters was done with 50 µl of reaction buffer. In the colloidal gold detection system, washing was done with 100 µl of reaction buffer. After the liquid absorption, the strips were dried in a 37 °C incubator with air flow for 30 min and measured after drying.

Fluorescence imaging by digital camera

The imaging of fluorescent Eu(III) nanoparticles on LF strips (Fig. 3A) was done by attaching the camera to a laboratory stand and a clamp at a height of 20 cm. The bandpass filter was attached to another clamp as close to the camera lens as possible. The imaging was done in a dark room, and the strips were illuminated by a handheld UV lamp. The exposure time of the camera was 15 s with aperture F3.4 and ISO sensitivity 200. This detection system represents a conventional fluorescence detection method with continuous excitation and measurement of reported specific signal through an optical bandpass filter.

Measurement and data interpretation

Maximum signals on binder surface area in fluorescence measurement scanning were compared, and the standard deviation (SD) of the replicate reactions was calculated. The images acquired with the imaging-based detection methods were initially processed using Corel Paint Shop Pro X2 software (Corel, Ottawa, Canada). The initial processing included cropping and resizing of assay strip images to a manageable size. The intensity profiles of the assay strip images were calculated by using the plot profile function of ImageJ software (National Institutes of Health, Bethesda, MD, USA). In both imaging methods, intensity signals on the binder surface area were summed and compared with an equally sized area of background signal. This signal-to-baseline ratio was used to measure the response of analyte. In scanning methods, signal integration was not done because the reading area of the scanning beam was large enough to cover the whole binding surface area of the strip. The cutoff level for all detection systems was calculated by the following equation:

$$3 * \mathrm{SD}\ (\text{background}) + \text{average background}).$$

The analytical sensitivity was calculated by fitting the measurement data with a linear model and reading the concentration of analyte at the cutoff level. Maximal signal-to-noise (S/N) ratios were calculated for each assay by dividing the maximum signal of the test line by the SD of the signals from the membrane area outside the binder surface.

Effect of human serum in background signal of fluorescence measurement

Lateral flow strips with human serum were measured with delayed time-resolved detection and an instant detection mode (Fig. 2) to compare the background signal originating from biological material without added reporters. The LF strips were measured after 100 µl of human serum was completely absorbed and dried.

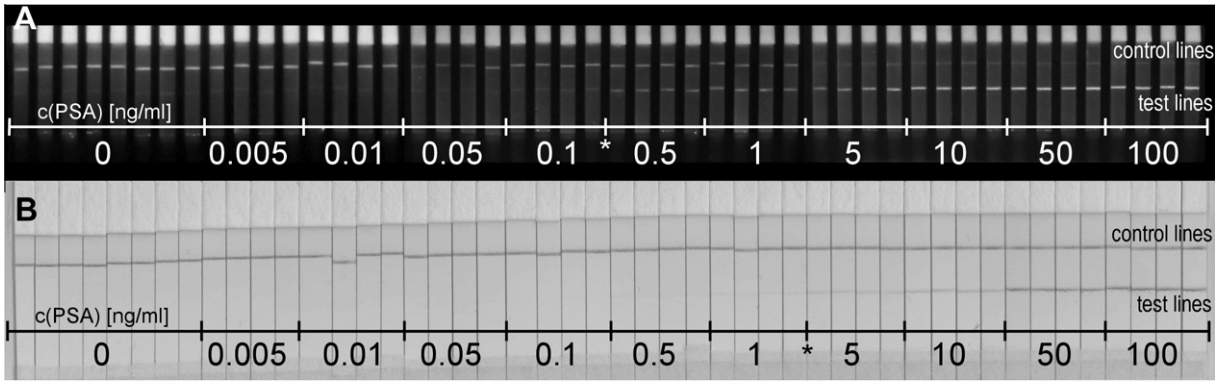

Fig.3. Photos of PSA strips from imaging-based detection methods. (A) Fluorescence image of strips with Eu(III) nanoparticles. (B) PSA strips with colloidal gold. Strips from left to right are in order of increasing PSA concentrations (range = 0–100 ng/ml). Analytical sensitivities at intervals between PSA concentrations are marked with a star.

Table 1
Matrix for optimization of LF assay conditions.

Nitrocellulose wicking rate (s/4 cm):	90	120	180[a]
10 mM buffer base	Tris	Hepes[a]	Na_2HPO_4/NaH_2PO_4
NaCl concentration (mM)	130	270[a]	
BSA (%, w/w)	0–2[b]		
Triton X-100 concentration (%, v/v)	0–0.5[c]		
Tween 20 concentration (%, v/v)	0–1[d]		

[a] Conditions with highest sensitivity obtained.
[b] Concentration range was tested, and 1% was found to be optimal.
[c] Concentration range was tested, and no effect was observed.
[d] Concentration range was tested, and 0.5% was found to be optimal.

As controls, 100 µl of previously mentioned assay buffer was absorbed. The assay comparison was done with five replicate strips and measured after drying the strips for 30 min at 35 °C. Measurements were done with Victor X4. The delayed time-resolved mode was done with a 400-µs delay time, a 400-µs counting window, and a duty cycle of 1000 µs. The instant detection measurement was done without any delay, with a 400-µs counting window and a 1000-µs duty cycle.

Results and discussion

Assay principle

The two model assays were optimized with respect to analytical sensitivity with both types of reporter particles. The performance of fluorescent Eu(III) particles was studied with three methods: delayed time-resolved scanning, instant detection fluorescence scanning, and photography through optical bandpass filter (Fig. 3A). The results were compared with reflectance-based scanning of colloidal gold particles (Fig. 3B).

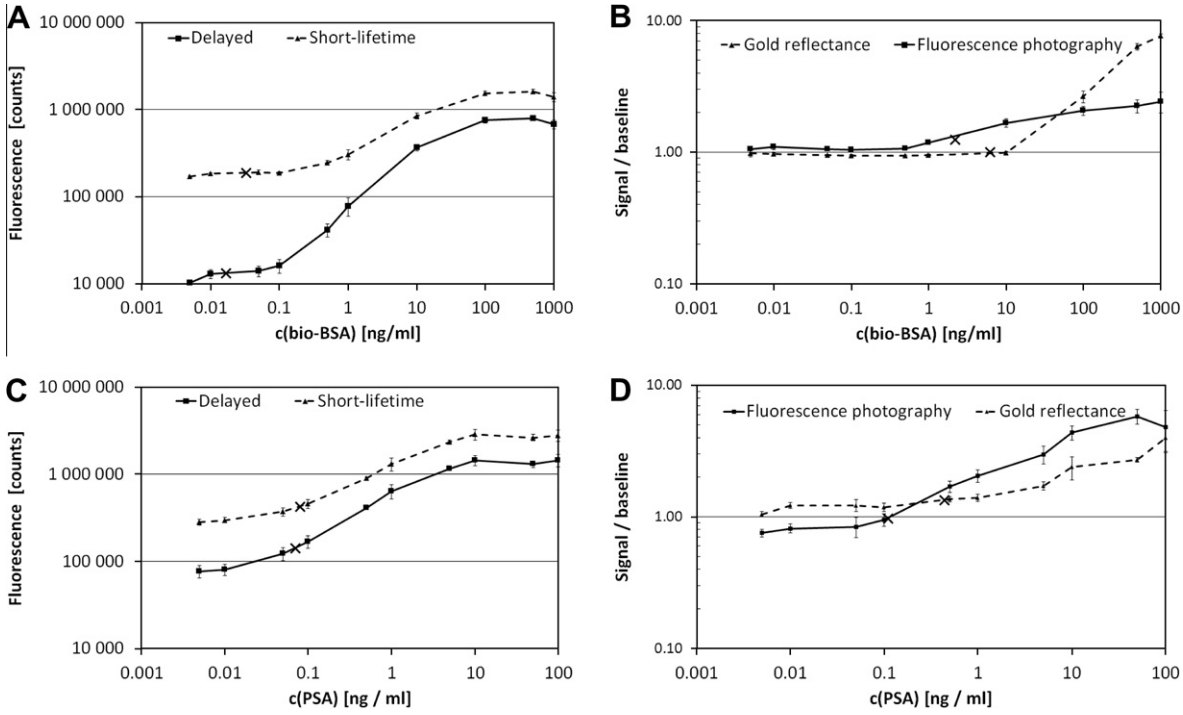

Fig.4. Dose–response graphs of PSA and bio-BSA in their respective assays. (A and C) Assays with scanning-based detection systems. Delayed time-resolved measurement is shown with solid line, and short-lived measurement is shown with dashed line. (B and D) Assays with imaging-based detection systems. Fluorescence photography shown with solid line and gold reflectance measurement with dashed line. Standard deviations in both directions are depicted as error bars. The limit of detection is marked with "×" in each curve.

Table 2
Analytical sensitivities of PSA assay and bio-BSA assays with compared detection methods.

	PSA assay sensitivity (ng ml^{-1})	Bio-BSA assay sensitivity (ng ml^{-1})
Colloidal gold	0.44	6.10
Delayed Eu measurement	0.07	0.02
Short lifetime Eu measurement	0.08	0.03
Fluorescence photography	0.11	2.21[a]

[a] Resulted from elevated background fluorescence.

The LF strip used in comparison of reporters consisted of nitrocellulose membrane, feeding pad, and absorption pad attached on a backing plastic (Fig. 1A). In the assay procedure, the liquids were sequentially absorbed in the test strip from microtiter wells (Fig. 1B). The first well of the sequence contained the analyte (bio-BSA or PSA). The second well contained the reporter particles (SA–Au or SA–Eu in bio-BSA assay and anti-PSA–Au or anti-PSA–Eu in PSA assay). The third well contained reaction buffer to wash the unbound reporters from the membrane. In this test format, the analyte molecule was first bound to the immobilized binder surface with subsequent introduction of the reporters (Fig. 1C). The sequential absorption of analyte and reporter was done to avoid cross-linking of SA-coated reporter particles by multivalent binding of bio-BSA. Such binding of reporters would result in the formation of reporter aggregates on the test strip.

The time needed to absorb all of the liquids through the nitrocellulose membrane was 30 to 40 min, and the total time (including the drying and measurement) resulted in a total assay time of 1 to 1.5 h. The sequential absorption of liquids was selected to serve the needs of assay development and component optimization but is not feasible in a real diagnostic LF assay. The analytical sensitivities of the bio-BSA model assays with the two reporters are comparable only with the same batch of bio-BSA because the biotinylation degree may vary in different experiments. The PSA assay offers a practically more relevant comparison because the analyte used is equal to the real analytical target, PSA produced in a baculovirus expression system [23].

Reaction composition optimization

Numerous buffers and reaction conditions were tested for both reporter systems (Table 1). The ones producing the highest sensitivity for a reporter system were chosen. The optimal buffer composition depends on multiple attributes in LF assay (e.g., the

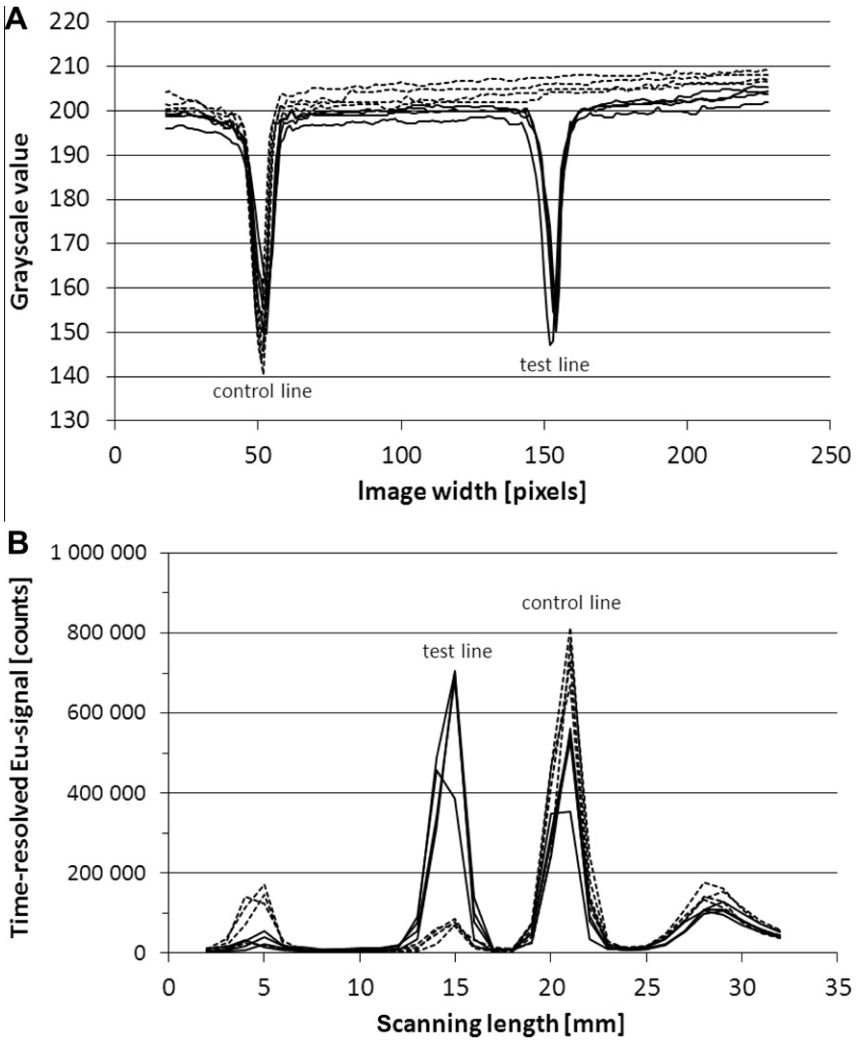

Fig.5. Examples of signal profiles of PSA with reflectometric measurement of colloidal gold (A) and delayed time-resolved fluorescence scanning of Eu(III) nanoparticles (B). Reactions with maximal signal (100 ng/ml PSA) are depicted with solid line, and reactions containing no analyte are depicted with dashed line. Both reactions are presented with four replicates.

Table 3
Evaluation of maximal signal-to-noise ratios obtained from strips ($n = 48$) with different detection methods.

	PSA assay				Bio-BSA assay			
	Background signal range	Median	SD	S/N ratio[a]	Background signal range	Median	SD	S/N ratio[a]
Colloidal gold[b]	198–207	202	1.7	70	225–235	231	1.8	131
Delayed Eu measurement[c]	3330–12641	6834	1893	372	4776–14234	7530	1839	454
Short lifetime Eu measurement[c]	148620–183249	159366	6987	207	148014–194344	166648	8240	207
Fluorescence photography[b]	52–92	70	11.3	18	85–145	119	11.2	21

[a] S/N, signal-to-noise ratio. Standard deviation (SD) of the background signal was considered as the noise.
[b] Background fluorescence in grayscale values.
[c] Background fluorescence in fluorescence counts.

membrane porosity and the properties of analyte molecule). Thus, the rationale of the buffer optimization was to minimize any unspecific binding between reporter particles and assay materials without compromising the signal intensities. Both reporter technologies required detergent, at least 0.1% Tween 20 in the buffer, to enable the reporters to move through the nitrocellulose membrane. The amount of SA–Eu and anti-PSA–Eu was tested in the range of 10^3 to 10^8 particles in the reaction, with 10^6 particles per reaction providing the maximal signal-to-background ratio. Different dilutions of the SA–Au particle stock solution (optical density of 0.715 AU at 520 nm) were tested. A 1:2 dilution showed no effect in bio-BSA dose–response, whereas the 1:4 dilution produced a visible decrease of the signal.

Comparison of analytical performance

Analytical sensitivities with each detection method were compared by analyzing dose–response curves of both analytes (Fig. 4). The sensitivities of both assays with each detection method were compared (Table 2). The reflectometric detection of colloidal gold was seen to be prone to errors caused by scratches, dust, and other physical artifacts in the measurement. In practical situations, such interfering factors lead to less reliable results. The scanning profiles (Fig. 5) shows that the signal peaks are measured at the correct position of the membrane surface. In addition, the background noise of the detection system is visible in the scanning profile of SA–Au (Fig. 5A). With the fluorescence photography detection, the analytical sensitivity of the PSA assay was 0.11 ng/ml. This demonstrates that the improvement gained with time-resolved detection is not significant in cases where the background signal originating from the unspecific binding of reporters is substantial. Technical limitations of the imaging experiment were considered in terms of detection sensitivity and reliability. In the case of the PSA assay, the camera was able to detect even the reporters bound on the binder surface without any analyte present (see dataset in supplementary material). Therefore, the sensitivity of the detection was not the limiting factor of the assay performance. However, in the case of the bio-BSA assay, an issue with the detection system reliability was observed. The photography was repeated due to failure of the UV lamp the first time. An unexpected effect of UV radiation on the reaction strips was observed. The background fluorescence of the nitrocellulose membrane was elevated during the UV radiation exposure. This, in combination with photobleaching of the reporters, resulted in lower assay sensitivity (2.21 ng/ml). Because of this bias, the result of the fluorescence photography of the bio-BSA assay is not considered to represent the optimal performance of the detection system.

The S/N ratios with each detection method were compared (Table 3). The background fluorescence was measured from the area adjacent to test line with 1 to 2 mm distance from the line. Thus, the background signal is considered to represent the measurement noise of the assay. The visual examination of the colloidal gold particles was in accordance with the results of reflectometric scanning measurement (Fig. 3B). The lowest visually detectable analyte concentrations were 10 ng/ml bio-BSA and 0.5 ng/ml PSA. A detection system using Eu(III)-coupled silica particles has been reported yielding a 100-fold increase in sensitivity over colloidal gold, although the time-resolved detection mode was not used [20]. This is in accordance with results described by this study. Improvement of detection sensitivity by delayed time resolution could not be seen with analytical sensitivities of the assays. This is mainly because there was unspecific binding of the reporters producing time-resolved fluorescence of 70,000 counts at the test area. Of that background signal, the proportion of the test materials is only 7000 counts. However, a beneficial effect of the delayed measurement mode could be seen by comparing the signals measured outside the test line (position 9–11 mm in Fig. 5B) (Table 4). At this position, the background signal originates mainly from the nitrocellulose membrane. Hence, the theoretical benefit from the time-resolved measurement mode is in direct proportion to the extent whereby the nonspecific binding of the Eu reporters can be diminished.

Table 4
Effect of time resolution delay on S/N ratio and interference from serum.

	Delayed Eu measurement signals	Short lifetime Eu measurement signals
Average maximum signal	1449779 (244111)	2805637 (427219)
Average signal of the nitrocellulose	7093 (1812)	165724 (7968)
S/N ratio[a]	204	17
Average signal with serum	7573 (4133)	391403 (33029)
Average signal with buffer	1994 (92)	155444 (4708)
Signal ratio (serum/buffer)	3.8	2.5

Note: Standard deviations of signals are in parentheses.
[a] Calculated from average maximum signal and average signal of the nitrocellulose.

Effect of human serum on background signal of fluorescence measurement

The potential to eliminate background fluorescence originating from the biological material itself with delayed time-resolved measurement was evaluated by comparing LF strips subjected to serum and buffer, respectively. The signals obtained with both measurement modes from nitrocellulose area were compared using five replicate strips (Table 4). Thus, there is no significant difference in the proportional increase of fluorescence caused by serum using the two measurement modes. The performance comparison assays were done with buffer-based calibrators containing no serum because optimal conditions for studying the detectability of the reporters were desired. This experiment suggested that the proportion of short-lived unspecific fluorescence has little effect

on the background signal when a pulsed excitation is used to measure Eu(III) nanoparticles.

Conclusions

In terms of analytical sensitivity, the fluorescent Eu(III) nanoparticles were shown to provide LF assays of highly improved performance with both of the model assays studied. Compared with the reflectometric measurement of colloidal gold, the fluorescence measurement of Eu(III) nanoparticles yielded 7-fold higher sensitivity in the PSA assay and 300-fold higher sensitivity in the bio-BSA assay. This difference suggests that the performances of the two reporters can vary with different assays and binder molecules. The scanning measurements on Eu(III) nanoparticles were proved to be most robust (i.e., insensitive to physical factors resulting in errors in measurement such as room dust and fibers from clothing).

Measurement noise originating from the detection system was compared with both reporters. Therefore, S/N ratios were also calculated. The very high S/N ratio obtained by scanning of Eu(III) nanoparticles demonstrated the robustness of the fluorescence measurement. Compared with S/N ratios obtained with colloidal gold, the Eu(III) nanoparticles were superior.

The use of the time-resolved detection mode in LF assays currently requires access to large-sized expensive fluorometers. As shown with the two model assays of this study, the instant detection mode provided approximately equal assay performance as the delayed time-resolved mode. Even with serum samples, which are considered to be complex biological materials potentially contributing to the short-lived fluorescence background, the instant detection mode measurement performed equally well. The long lifetime of the Eu(III) nanoparticle-derived fluorescence and the signal enhancement these reporters provide, in comparison with individual molecular fluorescent chelates, decrease the sensitivity-limiting effect of short-lived unspecific fluorescence of assay materials. Therefore, pulsed excitation without a delay before the photon counting time window still enables high detection sensitivities to be obtained using Eu(III) nanoparticle reporters. With continuous excitation, the specificity of Eu(III) nanoparticle reporters is based on the large Stokes shift that enables the exclusion of unspecific fluorescence by optical bandpass filters. Importantly, however, it should still be kept in mind that the time-resolved mode is of significant value for reaching lower detection limits when the nonspecific binding of the reporters can be decisively reduced in comparison with the prompt fluorescence-generating background mechanisms.

In many point-of-care applications (e.g., acute coronary syndromes), assays with very high analytical sensitivity and short turnaround times are highly appreciated. In such a context, the lack of affordable simple instrumentation, however, may constitute a limitation. Although a portable device for time-resolved fluorescence detection of LF assays has already been described, there are currently no commercially available portable readers for time-resolved fluorometry [19]. Eu(III) chelates require high-energy excitation light at wavelengths below 400 nm [24]. Currently available light sources with adequate power, such as a xenon flash lamp and its power supply unit, make measuring instruments large and expensive.

The future prospects of LF assays using fluorometry are dependent on the development of new instrumentation technology. The fast progress of light-emitting diode (LED) technology and light detection cells is opening more possibilities in miniaturization of time-resolved fluorescence detection instruments [25]. In addition, an alternative method using fluorescent lanthanide compounds, upconverting phosphor technology, could potentially provide a sensitive detection technology enabling simpler instrumentation design than with time-resolved fluorometry [26]. High-activity lanthanide reporters have great potential for improving the performance of LF assays.

Acknowledgments

This work was funded by TEKES, the National Technology Agency of Finland, under Grant 40388/09. Lateral flow assay membranes, backing plastics and colloidal gold solution, were kindly provided by Ani Biotech Oy (Vantaa, Finland).

Appendix A. Supplementary material

Supplementary data associated with this article can be found, in the online version, at http://dx.doi.org/10.1016/j.ab.2012.06.005.

References

[1] G.A. Posthuma-Trumpie, J. Korf, A. van Amerongen, Lateral flow (immuno)assay: its strengths, weaknesses, opportunities, and threats—a literature survey, Anal. Bioanal. Chem. 393 (2009) 569–582.
[2] S.K. James, B. Lindahl, P. Armstrong, R. Califf, M.L. Simoons, P. Venge, L. Wallentin, A rapid troponin I assay is not optimal for determination of troponin status and prediction of subsequent cardiac events at suspicion of unstable coronary syndromes, Int. J. Cardiol. 93 (2004) 113–120.
[3] A.H.B. Wu, A.S. Jaffe, The clinical need for high-sensitivity cardiac troponin assays for acute coronary syndromes and the role for serial testing, Am. Heart J. 155 (2008) 208–214.
[4] J.H. Leuvering, P.J. Thal, M. van der Waart, A.H. Schuurs, Sol particle immunoassay (SPIA), J. Immunoassay 1 (1980) 77–91.
[5] A. van Amerongen, J.H. Wichers, L.B. Berendsen, A.J. Timmermans, G.D. Keizer, A.W. van Doorn, A. Bantjes, W.M. van Gelder, Colloidal carbon particles as a new label for rapid immunochemical test methods: quantitative computer image analysis of results, J. Biotechnol. 30 (1993) 185–195.
[6] R.B. Peck, J. Schweizer, B.H. Weigl, C. Somoza, J. Silver, J.W. Sellors, P.S. Lu, A magnetic immunochromatographic strip test for detection of human papillomavirus 16 E6, Clin. Chem. 52 (2006) 2170–2172.
[7] Q. Xu, H. Xu, H. Gu, J. Li, Y. Wang, M. Wei, Development of lateral flow immunoassay system based on superparamagnetic nanobeads as labels for rapid quantitative detection of cardiac troponin I, Mater. Sci. Eng. 29 (2009) 702–707.
[8] Z. Li, Y. Wang, J. Wang, Z. Tang, J.G. Pounds, Y. Lin, Rapid and sensitive detection of protein biomarker using a portable fluorescence biosensor based on quantum dots and a lateral flow test strip, Anal. Chem. 82 (2010) 7008–7014.
[9] P. Corstjens, M. Zuiderwijk, A. Brink, S. Li, H. Feindt, R.S. Niedbala, H. Tanke, Use of up-converting phosphor reporters in lateral-flow assays to detect specific nucleic acid sequences: a rapid, sensitive DNA test to identify human papillomavirus type 16 infection, Clin. Chem. 47 (2001) 1885–1893.
[10] J. Yoo, Y.M. Jung, J.H. Hahn, D. Pyo, Quantitative analysis of a prostate-specific antigen in serum using fluorescence immunochromatography, J. Immunoassay Immunochem. 31 (2010) 259–265.
[11] G. Rundstrom, A. Jonsson, O. Mårtensson, I. Mendel-Hartvig, P. Venge, Lateral flow immunoassay using europium(III) chelate microparticles and time-resolved fluorescence for eosinophils and neutrophils in whole blood, Clin. Chem. 53 (2007) 342–348.
[12] L. Li, L. Zhou, Y. Yu, Z. Zhu, C. Lin, C. Lu, R. Yang, Development of up-converting phosphor technology-based lateral-flow assay for rapidly quantitative detection of hepatitis B surface antibody, Diagn. Microbiol. Infect. Dis. 63 (2009) 165–172.
[13] A. Nabatiyan, M.A. Baumann, Z. Parpia, D. Kelso, A lateral flow-based ultrasensitive p24 HIV assay utilizing fluorescent microparticles, J. Acquired Immune Defic. Syndr. 53 (2010) 55–61.
[14] H. Härmä, T. Soukka, T. Lövgren, Europium nanoparticles and time-resolved fluorescence for ultrasensitive detection of prostate-specific antigen, Clin. Chem. 47 (2001) 561–568.
[15] L. Kokko, T. Lövgren, T. Soukka, Europium(III)-chelates embedded in nanoparticles are protected from interfering compounds present in assay media, Anal. Chim. Acta 585 (2007) 17–23.
[16] J.U. Eskola, T.J. Nevalainen, T.N. Lövgren, Time-resolved fluoroimmunoassay of human pancreatic phospholipase A2, Clin. Chem. 29 (1983) 1777–1780.
[17] I. Hemmila, Lanthanides as probes for time-resolved fluorometric immunoassays, Scand. J. Clin. Lab. Invest. 48 (1988) 389–399.
[18] E.P. Diamandis, T.K. Christopoulos, Europium chelate labels in time-resolved fluorescence immunoassays and DNA hybridization assays, Anal. Chem. 62 (1990) 1149A–1157A.
[19] X. Song, M. Knotts, Time-resolved luminescent lateral flow assay technology, Anal. Chim. Acta 626 (2008) 186–192.

[20] X. Xia, Y. Xu, X. Zhao, Q. Li, Lateral flow immunoassay using europium chelate-loaded silica nanoparticles as labels, Clin. Chem. 55 (2009) 179–182.
[21] K. Pettersson, T. Piironen, M. Seppälä, L. Liukkonen, A. Christensson, M.T. Matikainen, M. Suonpää, T. Lövgren, H. Lilja, Free and complexed prostate-specific antigen (PSA): in vitro stability, epitope map, and development of immunofluorometric assays for specific and sensitive detection of free PSA and PSA–α_1-antichymotrypsin complex, Clin. Chem. 41 (1995) 1480–1488.
[22] T. Soukka, H. Härmä, J. Paukkunen, T. Lövgren, Utilization of kinetically enhanced monovalent binding affinity by immunoassays based on multivalent nanoparticle–antibody bioconjugates, Anal. Chem. 73 (2001) 2254–2260.
[23] K. Rajakoski, T. Piironen, K. Pettersson, J. Lövgren, M. Karp, Epitope mapping of human prostate specific antigen and glandular kallikrein expressed in insect cells, Prostate Cancer Prostatic Dis. 1 (1997) 16–20.
[24] E.P. Diamandis, Immunoassays with time-resolved fluorescence spectroscopy: principles and applications, Clin. Biochem. 21 (1988) 139–150.
[25] D. Stoppa, D. Mosconi, L. Pancheri, L. Gonzo, Single-photon avalanche diode CMOS sensor for time-resolved fluorescence measurements, IEEE Sens. J. 9 (2009) 1084–1090.
[26] A.L. Ouellette, J.J. Li, D.E. Cooper, A.J. Ricco, G.T. Kovacs, Evolving point-of-care diagnostics using up-converting phosphor bioanalytical systems, Anal. Chem. 81 (2009) 3216–3221.